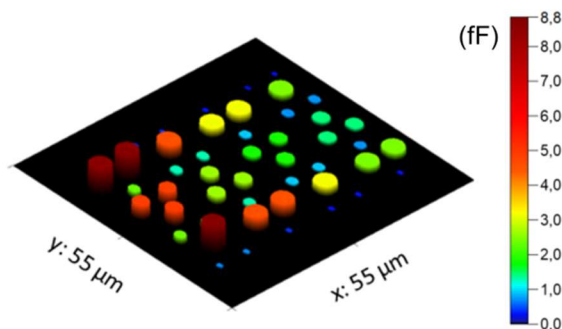




Good practice guide for calibrated capacitance measurements using scanning microwave microscopy



Abstract

Within the EMPIR project ADVENT, several European National metrology institutes perform researches on the development of nanometrology adapted to the new classes of materials proposed for the next generation of ultra-low power energy-efficient devices. One of the tasks focused on the development of calibration methods for nanoscale impedance measurements using scanning microwave microscopes (SMM). In this report, LNE with the support of METAS proposes a good practice guide to carry out SMM based capacitance measurements traceable to the international system of units (SI).

Content

- 1. Introduction..... 3
- 2. Experimental section 3
 - 2.1.SMM system..... 3
 - 2.2.Environmental conditions 4
 - 2.3.SMM operation conditions 4
 - 2.4.Measurement principle..... 4
 - 2.5.References devices..... 5
 - 2.6.SMM calibration method 6
- 3. Measurement Procedure..... 6
 - 3.1.Calibration of SMM 6
 - 3.2.Uncertainty budget 7
 - 3.3.Procedure of capacitance calibration 7
- 4. Calibration results..... 8

1. Introduction

In the framework of EURAMET's funding initiative European Metrology Programme for Innovation and Research (EMPIR), the project ADVENT (Advanced Energy – Saving Technology) establishes the metrology required for this transformational objective for Europe by providing traceable measurements of power, losses and electronic properties of emerging materials. One part of the project focused on the development of a broad metrology platform to extend the spatial resolution of material characterization techniques and compositional measurement down to the nanometer scale, to quantify impedance of novel materials with an uncertainty below 10 %, and to extend measurement of stress and strain responses to electric field up to 4 MV/cm and magnetic field up to 2 T. This good practice guide (GPG) summarizes the use of scanning microwave microscopy (SMM) as a relevant technique for carrying out nanoscale capacitance measurements with a demonstrated traceability to the international system of units (SI). This GPG was established by LNE with the support of METAS. The two NMIs currently develop nanoscale impedance metrology using two types of SMM, cantilever based SMM (LNE) and tuning-fork based SMM (METAS).

In the following sections, we give a general description of the experimental set-up, detail the calibration method developed for nanoscale capacitance measurements based on SMM, and present the calibration results on micrometer sized capacitors together with the main contributions to the uncertainty budgets.

2. Experimental section

2.1. SMM system

A SMM consists of a scanning probe microscope (SPM), an atomic force microscope (AFM) (in both NMIs) or a scanning tunneling microscope, and a vector network analyzer (VNA). The conductive SMM tip of the SMM is connected to the microwave source/meter of VNA (see Fig.1). While the tip scans over the sample surface, it irradiates the microwave signal, highly localized at the apex, over a local region of the sample, allowing simultaneous topographic and electrical characterization of the sample under study. Depending on the mismatch between the characteristic impedance (Z_0) and the local impedance of the tip-sample system (Z_s), one part of the incident microwave signal is reflected back travelling from the tip-sample contact point to the VNA and the other part is transmitted throughout the sample. The ratio between the reflected and incident signals, the so-called S_{11} scattering parameter, is then measured by the VNA and converted into complex impedance values following the one-port VNA calibration procedure (see part 3.1) [1]. The numerical value of S_{11} measured in dB is obtained as $20 \cdot \log(a_{ref}/a_{inc})$, where a_{ref} and a_{inc} are the reflected and incident wave signals at the tip/surface interface, respectively.

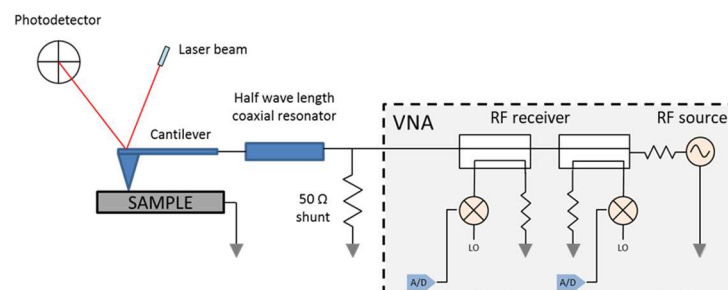


Figure 1. Schematic diagram of the AFM-based SMM setup, where the AFM part stays on the left and the VNA part stays on the right.

2.2. Environmental conditions

Similar to a conventional SPM set up, the whole SMM is supported by anti-vibration systems to damp down mechanical vibrations. A Faraday chamber would also suppress additional electromagnetic signals from surroundings during SMM measurements. Furthermore, it is important to control well the measurement conditions (temperature, humidity, light and others). For this purpose, the whole SMM setup can be placed in a glove box. Figure 2 shows the SMM microscope installed at LNE in a glove box under a dry nitrogen atmosphere ($RH < 1\%$) and at room temperature ($T = 24.3\text{ }^{\circ}\text{C} \pm 0.1\text{ }^{\circ}\text{C}$).



Figure 2. SMM setup at LNE, where the AFM part is located in a glove box.

2.3. SMM operation conditions

Imaging conditions - SMM images are best acquired in contact mode, where the tip remains in contact with measured surface during the whole measurement process and ensures a homogenous electrical contact. Recorded signals consists of topography and electrical data ($S_{11,m}$ -Magnitude and $S_{11,m}$ -Phase).

Choice of the VNA operating frequency - Before landing the SMM probe on the sample surface, a full frequency sweep of VNA signal is performed over its operation frequency range with a tip hovering above the sample surface but not in contact yet. The microwave frequency with the lowest $S_{11,m}$ - Magnitude signal is chosen for resonance based impedance matching systems.

Image processing - During SMM scanning, a linear drift can be observed from the raw $S_{11,m}$ data (Magnitude and Phase) in the slow scan Y-direction. The drift can result from the non-null synchronization time interval between VNA measurements and the AFM topography, both acquired line by line. The drift can also be due to the thermal expansion characteristics of interconnecting cables within the test set. It is important to take this parasitic effect into account for the image processing. To get rid of this drift, the raw $S_{11,m}$ images are processed by taking into account instead the raw data of measurements of the difference $\Delta S_{11,m} = S_{11,m}^C - S_{11,m}^{Si}$ by subtracting the raw $S_{11,m}^{Si}$ signals measured on Si substrate from the raw $S_{11,m}^C$ signals measured on individual capacitors, line by line. This image processing on raw $S_{11,m}$ maps has also the advantage to null or at least make negligible the errors due to parasitic capacitors occurring in parallel to the microcapacitors under study, such as capacitor between unshielded parts of the SMM and the Si substrate.

2.4. Measurement principle

The capacitance measurement method proposed here only applies to samples of micrometer or nanometer size capacitors and to the microwave domain. The microcapacitors are composed of a dielectric thin layer (made of material under investigation) sandwiched between a top metal electrode and a conducting substrate (a metal or a highly doped semiconductor) forming a back

electrode. Their capacitances are measured using a cantilever-based SMM, as shown in Fig.3. The sample is positioned under the conductive SMM tip and very close to the reference device which serves to calibrate the SMM in terms of capacitance. Once the calibration is done, the reference device is substituted by the sample. This substitution method allows one to preserve the SMM calibration data [2].

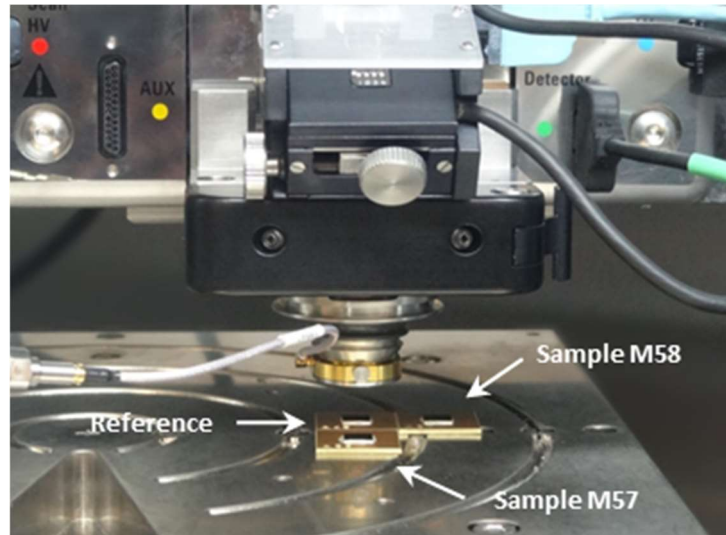


Figure 3. Reference calibration kit (in the centre) and two samples (M57, M58) to be calibrated.

2.5. References devices

A calibration kit fabricated by MC2 Technologies is used to calibrate the SMM. As shown in Fig.4, each $45 \times 45 \text{ mm}^2$ substrate has 144 identical $140 \times 140 \text{ }\mu\text{m}^2$ pads. Each pad has 4 identical sets of 48 microcapacitors. Each capacitor consists of a circular gold electrode (gold pad height = 281 nm) deposited on silicon dioxide with different thicknesses and a Si (100) substrate strongly doped with boron atoms (p-type) (Fig.5). The doping concentration N_a of the substrate is sufficiently high ($N_a = 7.98 \times 10^{18} \text{ atoms/cm}^3$), so that for each device, its parasitic depletion capacitance C_d remains negligible compared to its dielectric capacitance C_{ox} . Thanks to the variation of SiO_2 thickness (from 50 nm to 220 nm with about 50 nm steps) and the lateral size of the gold electrode (with diameters varying from 1 μm to 4 μm), capacitance values of fabricated microcapacitors vary from 100 aF to 10 fF. More details about the fabrication process of calibration sample are described elsewhere [3].

It must be noted here that the knowledge of the capacitance values results from calculation using the measured values of the dimensional parameters of the capacitors (thickness of the dielectric layer and the area of the top electrode). These parameters can be measured with certain uncertainty by AFM or scanning electron microscope (SEM) techniques. The capacitance calculations also depend on the relative permittivity ϵ_r value of the silicon dioxide, usually set to 3.9 as nominal value [4][5]. These calculations, relying on an analytical approach or use a finite element modeling, take into account the effects of fringing fields.

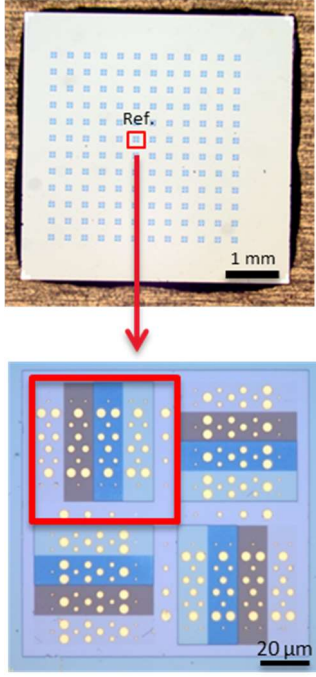


Figure 4. Top: a top view optical image of one of the used calibration sample. In this image, the pad, where the device set were used for the calibration, is labelled and marked. Below: a zoom in optical image of the same pad and the chosen set is framed in red square.

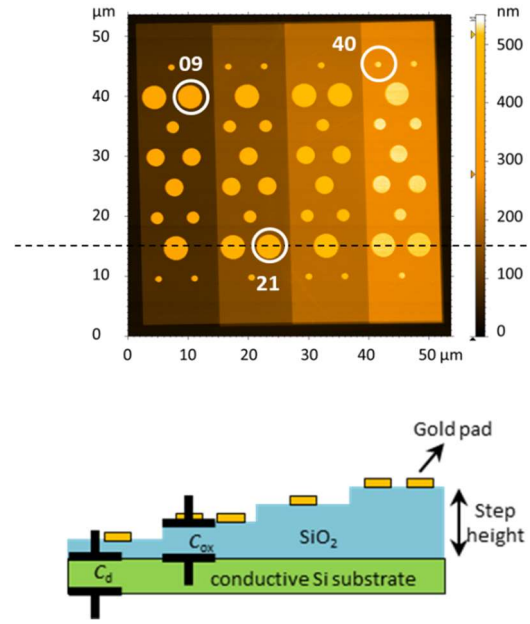


Figure 5. Top: AFM image of an area where all 48 microcapacitors stay. Below: cross section view taken along the dashed line shown in the top panel. The scale is not proportional.

2.6. SMM calibration method

The calibration of the SMM consists in converting the raw measured reflection coefficient $S_{11,m}$ into the complex impedance of the sample under study Z_s using the modified Short Open Load (SOL) calibration method proposed by Hoffmann *et al* [1]. The quantities $S_{11,m}$ and Z_s are related by two equations:

$$S_{11} = \frac{Z_s - Z_r}{Z_s + Z_r} \quad (1)$$

$$S_{11,m} = e_{00} + e_{01} \left(\frac{S_{11}}{1 - e_{11} S_{11}} \right) \quad (2)$$

where S_{11} is the expected reflection coefficient and e_{00} , e_{01} , and e_{11} are three complex parameters (also known as error parameters) to be determined from $S_{11,m}$ measurements on three reference structures with known capacitance values. Z_r is a non-zero reference impedance, which can be chosen arbitrarily. It is important to note that this calibration requires all measurements (for reference and DUT devices) to be performed with the same tip and at the same RF frequency. The whole calibration process needs to be repeated to calibrate the SMM measurement at other frequencies.

3. Measurement Procedure

3.1. Calibration of SMM

The calibration of SMM requires at least three capacitors with known capacitance values. A poor and arbitrary selection of these three capacitors without established criteria can lead to obtain

erroneous results on capacitance measurements after SMM calibration. The capacitors of the reference device are selected according to the following criteria:

- they present a really clean surface confirmed by AFM;
- they insure a good and homogeneous electrical contact between the SMM tip and their top electrode;
- their capacitances satisfy approximately the inequality $|C_i - C_j| \geq \Delta C_{\max}/2$,

where i and j ($\neq i$) ranging from 1 to 48 and ΔC_{\max} is the difference between the highest and lowest capacitance values $\Delta C_{\max} = C_{\max} - C_{\min}$. Depending on the capacitance value of the device under test (DUT), it is important to choose a triplet of capacitors, the range of which covers the expected value of the DUT. For example, for the DUT with a capacitance around 0.1 fF, a triplet with capacitances around 0.1 fF, 1 fF and 10 fF would be more suitable than the one with capacitances around 1 fF, 5 fF and 10 fF.

3.2. Uncertainty budget

The uncertainty on the SMM calibration essentially depends on the uncertainties corresponding to the calculated capacitance values of the selected capacitor triplet. These are composed of the uncertainties on the measurements of the top electrode areas (measurement repeatability, pitch AFM calibration, and tip profile determination) and on the measurements of the SiO₂ layer thickness (repeatability and height AFM calibration). The uncertainty values thus depend on the performances of the AFM used to measure the dimensional parameters of the capacitor and on the instruments used to dimensionally calibrate this AFM. In the most favorable case, the relative standard uncertainties could be reduced down to a few percents ($k = 1$). Four other uncertainty contributions can be considered but have a minor impact on the budget. The first is related to the depletion capacitance effect and does not exceed 3 parts in 10⁴ in the case of the MC2 reference device. The second uncertainty contribution comes from the uncertainty of the relative permittivity of the silicon dioxide. An uncertainty in the order of 1 part in 10³ can be reached from split-cylinder cavity techniques [6]. However this uncertainty has not yet been demonstrated in conjunction with SMM measurements. A conservative uncertainty value of 1% would be therefore taken into account. The third uncertainty contribution comes from moving SMM stage from reference structure to test structure. This contribution could be zero under certain conditions such as similar reference and test structures. This uncertainty can be evaluated by comparing results from different measurement constellations such as positioning the reference structure to the left, right, bottom or top of the test structure. The fourth uncertainty contribution is the effect of high frequency on the depletion capacitance. Depending on the used model, the measurement conditions (e.g. operating frequency) and the doping concentration of the Si substrate of the reference structure, this uncertainty would be in the order of a few percents.

3.3. Procedure of capacitance calibration

The sample composed of capacitors to be calibrated is positioned very close to the reference calibration kit as shown in Fig.3. The SMM is at first calibrated using the values of the capacitance triplet ($C_{\text{ref-high}}$, $C_{\text{ref-int}}$, $C_{\text{ref-low}}$) which has been beforehand selected and calculated from a chosen pattern of the reference calibration kit. The capacitances of the “unknown” sample are then calibrated by repeating 5 times the following measurement cycles:

- (i) Single topographic and capacitance image of all the 48 microcapacitors of the reference pattern to check the SMM calibration;
- (ii) Single topographic and capacitance image of the sample.

4. Calibration results

To demonstrate the powerful capability of the SMM to calibrate capacitances of capacitors at nanoscale with a guaranteed traceability to the SI by applying the substitution method proposed in this GPG, LNE has performed capacitance measurements on two “unknown” samples [2]. Those are calibration kits from MC2 Technologies labelled M57 and M58 which have same number of patterns and capacitors with similar configurations (four SiO₂ dielectric terraces of different thickness ...) as for the reference sample but came from different growth batches and do not have the same Si substrate (different doping levels). The calibrations were performed at the VNA working frequency of 3.808 6 GHz and the SMM was calibrated using the selected capacitor triplet (C_{ref-09} , C_{ref-21} , C_{ref-40}) (as shown in Fig.5).

The measured capacitance values have been found ranging from 0.1 fF to 3.1 fF (Fig.6) with a combined relative uncertainties varying from 14 % to 7 % respectively.

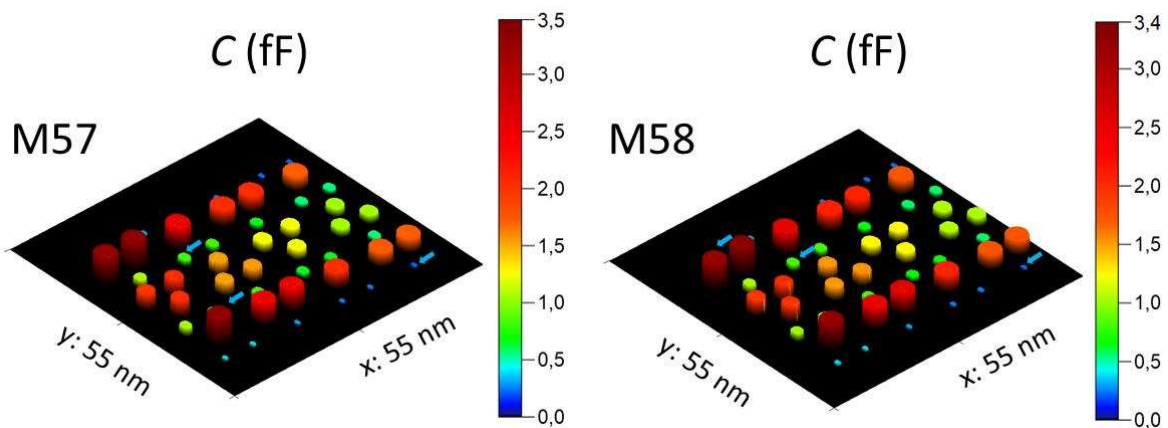


Figure 6. Calibrated capacitances on two samples M57 and M58.

Table 1 summarizes capacitance values and corresponding combined standard uncertainties for three particular capacitors from M57 ($C_{high-05}$, C_{int-15} , C_{low-44}) and M58 ($C_{high-01}$, C_{int-15} , C_{low-44}) samples.

The combined standard uncertainties result from the main uncertainty contributions that are summarized in Tab.2 below for M57 sample (similar values are found for M58 sample).

As expected, the largest contribution comes from the SMM calibration uncertainty. Details are given below. No change of the error parameters (e_{00} , e_{01} , and e_{11}) has been detected from the measurements carried out on the reference pattern. The repeatability levels observed on the measurements of C_{ref-09} , C_{ref-21} , and C_{ref-40} have been found between 0.04 % and 0.94 %.

In contrast, the repeatability of measurements performed on M57 and M58 samples is lower, ranging from 0.6 % to 3.6 % (see Tab.2). Finally, the uncertainty contribution from parasitic capacitances becomes non negligible for the smallest capacitance, reaching almost 5 %.

Table 1. Capacitances and standard uncertainties for 3 capacitors of samples M57 and M58.

C values (fF)	M57	M58
High	3.14 ± 0.21	3.13 ± 0.25
Intermediate	0.71 ± 0.06	0.71 ± 0.07
Low	0.15 ± 0.03	0.17 ± 0.03

Table 2. Main uncertainty contributions for 3 values measured on M57 sample: $C_{\text{high-05}}$ (3.14 fF), $C_{\text{int-15}}$ (0.78 fF), $C_{\text{low-44}}$ (0.20 fF).

Uncertainty budget for C_i	C_{high}	C_{int}	C_{low}
	(%)		
Repeatability	2.4	2.7	3.6
SMM calibration	6.3	7.8	13.4
Parasitic capacitances	0.2	0.9	4.5
<i>Stray capacitance</i>	0.0	0.4	3.5
<i>Water meniscus</i>	0.2	0.7	2.9
<i>Sample location</i>	<i>To be determined</i>		
Combined uncertainty u_{cm}	6.7	8.3	14.2

The SMM calibration uncertainty is estimated from the uncertainties of capacitance calculation of the selected capacitors $C_{\text{ref-09}}$, $C_{\text{ref-21}}$, and $C_{\text{ref-40}}$ given in Tab.3. The reported values of the top electrode area A and the SiO_2 layer thickness d have been measured from a series of 15 topography images.

Table 3. Calculated capacitances C_{calc} and measured top electrode area A and thickness d , of four capacitors with combined standard uncertainties u_C , u_A and u_d .

Capacitor	$C_{\text{calc}} \pm u_C$ (fF)	$A \pm u_A$ ($\mu\text{m} \times \mu\text{m}$)	$d \pm u_d$ (nm)
$C_{\text{ref-09}}$	8.57 ± 0.41	12.64 ± 0.28	55.8 ± 2.5
$C_{\text{ref-21}}$	4.42 ± 0.24	12.03 ± 0.28	106.1 ± 5.0
$C_{\text{ref-40}}$	0.18 ± 0.03	0.65 ± 0.09	212.0 ± 3.8

The combined standard uncertainties u_C , u_A and u_d result from the main uncertainty contributions that are summarized in Tab.4. AFM of the SMM set-up has been used to measure both the top electrode areas of the capacitors and the SiO_2 layer thickness.

Table 4. Main uncertainty contributions for the calculation of the selected capacitance standards.

Uncertainty budget for C_i calculation	$C_{\text{ref-09}}$	$C_{\text{ref-21}}$	$C_{\text{ref-40}}$
	(%)		
Area measurements, u_A	2.4	2.5	14.3
<i>Repeatability</i>	0.4	0.5	1.3
<i>Pitch AFM calibration</i>	0.9	0.9	0.9
<i>Tip profile</i>	2.2	2.3	14.2
Thickness measurements, u_d	4.4	4.7	1.8
<i>Repeatability</i>	4.3	4.6	1.6
<i>Height AFM calibration</i>	1.0	1.0	1.0
Depletion capacitance, u_{cd}	0.03	0.02	0.02
HF influence on Cd	1	1	1
Permittivity ϵ_r (SiO_2)	1	1	1
Combined uncertainty u_C	5.1	5.4	14.4

References

- [1] J. Hoffmann, M. Wollensack, M. Zeier, J. Niegemann, and H. Huber, "A Calibration Algorithm for Nearfield Scanning Microwave Microscopes," *12th IEEE Int. Conf. Nanotechnol. IEEE-NANO*, pp. 1–4, 2012.
- [2] J. Moran, A. Delvallée, D. Allal, and F. Piquemal, "A substitution method for nanoscale capacitance calibration using scanning microwave microscope," *Meas. Sci. Technol.*, vol. 31, no. 074009, 2020.
- [3] H. P. Huber *et al.*, "Calibrated nanoscale capacitance measurements using a scanning microwave microscope," *Rev. Sci. Instrum.*, vol. 81, pp. 113701, 2010.
- [4] M. K. Kazimierczuk, *Pulse-Width Modulated DC–DC Power Converters*, Second Edi. John Wiley & Sons, Ltd., 2016.
- [5] J. Robertson, "High dielectric constant oxides," *Eur. Phys. J. Appl. Phys.*, vol. 28, pp. 265–291, 2004.
- [6] M. D. Janezic, U. Arz, S. Begley, P. Bartley, A. Technologies, and S. Rosa, "Improved Permittivity Measurement of Dielectric Substrates by use of the TE₁₁₁ Mode of a Split-Cylinder Cavity," *73rd ARFTG Microw. Meas. Conf.*, pp. 1–3, 2009.